Low-mass dilepton rate from the deconfined phase

Carsten Greiner,[1] Najmul Haque,[2] Munshi G. Mustafa,[1,2] and Markus H. Thoma[3]
[1]*Institut für Theoretische Physik, Johann Wolfgang Goethe University, Max-von-Laue-Strasse 1, D-60438 Frankfurt, Germany*
[2]*Theory Division, Saha Institute of Nuclear Physics, 1/AF Bidhannagar, Kolkata 700 064, India*
[3]*Max-Planck-Institut für extraterrestrische Physik, Giessenbachstrasse, 85748 Garching, Germany*
(Received 13 October 2010; published 25 January 2011)

We discuss low-mass dilepton rates ($\leqslant$1 GeV) from the deconfined phase of QCD using both perturbative and nonperturbative models and compare them with those from lattice gauge theory and in-medium hadron gas. Our analysis suggests that the rate at very low invariant mass ($M \leqslant 200$ MeV) using the nonperturbative gluon condensate in a semiempirical way within the Green function approach dominates over the Born rate, independent of any uncertainty associated with the choice of the strong coupling in perturbation theory. On the other hand, the rate from ρ-q interaction in the deconfined phase is important at 200 MeV $\leqslant M \leqslant 1$ GeV as it is almost of same order as the Born rate as well as the in-medium hadron gas rate. Also, the higher order perturbative rate, leaving aside its various uncertainties, from the hard-thermal-loop approximation becomes reliable at $M \geqslant 200$ MeV and also becomes comparable with the Born rate and the lattice rate for $M \geqslant 500$ MeV, constraining on the broad resonance structures in the dilepton rate at large invariant mass. We also discuss the lattice constraints on the low-mass dilepton rate. Furthermore, we discuss a realistic way to advocate the quark-hadron duality hypothesis based on the dilepton rates from quark-gluon plasma and hadron gas.

DOI: 10.1103/PhysRevC.83.014908 PACS number(s): 12.38.Cy, 12.38.Mh, 25.75.Cj, 11.10.Wx

I. INTRODUCTION

The prime intention for ultrarelativistic heavy-ion collisions is to study the behavior of nuclear or hadronic matter at extreme conditions such as very high temperatures and energy densities. A particular goal lies in the identification of a new state of matter formed in such collisions, the quark-gluon plasma (QGP), where the quarks and gluons are deconfined from the nucleons and move freely over an extended space-time region. Various measurements taken at CERN's Super Proton Synchrotron (SPS) [1] and Brookhaven National Laboratory's Relativistic Heavy-Ion Collider (RHIC) [2–7] do lead to circumstantial evidence for the formation of QGP. Evidence is (and can only be) circumstantial because only indirect diagnostic probes exist.

Electromagnetic probes, such as real photons and dileptons, are a particular example, and accordingly thermal dileptons have been theoretically proposed a long time ago [8]. At SPS energies [9], there was an indication for an enhancement of the dilepton production at low invariant mass ($0.2 \leqslant M$ (GeV) $\leqslant 0.8$) compared to all known sources of electromagnetic decay of the hadronic particles and the contribution of a radiating simple hadronic fireball (for comprehensive reviews, see Refs. [10–12]). One of the possible explanations of this is the modification of the in-medium properties of the vector meson (viz., ρ meson) by rescattering in a hadronic phase along with only the lowest order perturbative rate, that is, $q\bar{q}$ annihilation from a QGP [10–13]. Also at RHIC energies [3], a substantial excess of electron pairs was reported in the low-invariant-mass region. Models taking into account in-medium properties of hadrons with various ingredients (see Refs. [14,15] for details) cannot explain the data from RHIC in the range $0.15 \leqslant M$ (GeV) $\leqslant 0.5$, whereas they fit the SPS data more satisfactorily, indicating that a possible nonhadronic source becomes important at RHIC.

On the other hand, the higher order perturbative calculations [16] also are not very reliable at temperatures within the reach of the heavy-ion collisions. Moreover, perturbative calculations of the dilepton rate seem not to converge even in a small coupling (g) limit. Nevertheless, the lowest order perturbative $q\bar{q}$ annihilation is the only dilepton rate from the QGP phase that is extensively used in the literature. However, this contribution should be dominant at large invariant mass but not at low invariant mass, where nonperturbative effects should play an important role. Unfortunately, the lattice data [17], because of its limitations, also could not shed any light on the low-mass dileptons. However, the lattice calculations [18–20] provide evidence for the existence of nonperturbative effects associated with the bulk properties of the deconfined phase, in and around the deconfined temperature, T_c. Also, indications have been found that the QGP at RHIC energies behaves more as a strongly coupled liquid than as a weakly coupled gas [21]. Thus, a nonperturbative analysis of the dilepton rate from the deconfined phase is essential.

The dilepton emission at low invariant mass from the deconfined phase is still an unsettled issue in heavy-ion collisions at SPS and RHIC energies and, in particular, would be an important question for LHC energies, compact baryonic matter formation in future Facilty for Antiproton and Ion Research (FAIR) energies [22], and the quark-hadron duality [10,11,23] that entails a reminiscence to a simple perturbative lowest order $q\bar{q}$ annihilation rate [24]. In this article, we reconsider the dilepton production rates within the perturbative QCD and nonperturbative models based on lattice inputs and phenomenological ρ-q interaction in the deconfined phase. The analysis suggests that the nonperturbative dilepton rates are indeed important at the low-invariant-mass regime.

This article is organized in the following way. In Sec. II, we discuss the dilepton production rate from the deconfined phase based on both perturbative and nonperturbative models.

In Sec. III, we compare the momentum integrated rates from both QGP and hadron gas (HG). We discuss the quark-hadron duality in Sec. IV and conclude in Sec. V.

II. DILEPTON RATE FROM DECONFINED PHASE

The dilepton production rate can be derived from the imaginary part of the photon self-energy [8,25] as

$$\frac{dR}{d^4x d^4P} = -\frac{\alpha}{12\pi^4}\frac{1}{e^{E/T}-1}\frac{\mathrm{Im}\Pi^{\mu}_{\mu}(P)}{M^2}, \tag{1}$$

where $\alpha = e^2/4\pi$, P is the four-momentum of the virtual photon, E is its energy, and we use the notation $P \equiv (p_0 = E, \vec{\mathbf{p}})$ and $p = |\vec{\mathbf{p}}|$. The square of the invariant mass of dilepton pair is $M^2 = p_0^2 - p^2$.

A. Born rate

To the lowest order, the dilepton rate follows from one-loop photon self-energy containing bare quark propagators. This rate corresponds to a dilepton production by the annihilation of bare quarks and antiquarks of the QGP. Alternatively, this so-called Born rate can also be obtained from the matrix element of the basic annihilation process folded with the thermal distribution functions of quarks. In the case of massless lepton pairs in a QGP with two massless quark flavors with chemical potential, one finds [24]

$$\frac{dR}{d^4x d^4P} = \frac{5\alpha^2}{36\pi^4}\frac{T}{p}\frac{1}{e^{E/T}-1} \times \ln\frac{(x_2+\exp[-(E+\mu)/T])(x_1+\exp[-\mu/T])}{(x_1+\exp[-(E+\mu)/T])(x_2+\exp[-\mu/T])}, \tag{2}$$

where $x_1 = \exp[-(E+p)/2T]$ and $x_2 = \exp[-(E-p)/2T]$. A finite quark mass can easily be included.

For $\mu = 0$, the dilepton rate becomes

$$\frac{dR}{d^4x d^4P} = \frac{5\alpha^2}{18\pi^4}\frac{T}{p}\frac{1}{e^{E/T}-1}\ln\left(\frac{\cosh\frac{E+p}{4T}}{\cosh\frac{E-p}{4T}}\right), \tag{3}$$

whereas that for total three-momentum $\vec{\mathbf{p}} = 0$ is given as

$$\frac{dR}{d^4x d^4P} = \frac{5\alpha^2}{36\pi^4}\, n(E/2-\mu)\, n(E/2+\mu), \tag{4}$$

with $n(y) = [\exp(y)+1]^{-1}$, the Fermi-Dirac distribution function.

B. Hard thermal loop perturbation theory (HTLpt) rate

To judge the reliability of the lowest order result, one should consider higher order corrections. These corrections involve quarks and gluons in the photon self-energy beyond the one-loop approximation. Using bare propagators at finite temperature, however, one encounters infrared singularities and gauge-dependent results. These problems can be resolved, at least partially, by adopting the hard-thermal-loop (HTL) resummation scheme [26]. The key point of this method is the distinction between the soft momentum scale ($\sim gT$) and the hard one ($\sim T$), which is possible in the weak coupling limit ($g \ll 1$). Resumming one-loop self-energies, in which the loop momenta are hard (HTL approximation), effective propagators and vertices are constructed, which are as important as bare propagators if the momentum of the quark or gluon is soft. In HTLpt, the bare N-point functions (propagator and vertices) are replaced by those effective N-point HTL functions that describe medium effects in the QGP such as the thermal masses for quarks and gluons and Landau damping.

The importance of the medium and other higher order effects on the dilepton rate depends crucially on the invariant mass and the momenta of the virtual photon. Therefore, we discuss now the different kinematical regimes:

1. Soft rate ($M \sim gT$ and $p \sim gT$)

For soft invariant masses[1] and momenta of order gT, one has to use HTL quark propagators and vertices in the one-loop photon self-energy. These corrections are of the same order as the Born term [28]. Physically, these corrections correspond to two different processes. First, the poles of the HTL resummed quark propagators describe quasiparticles in the QGP with an effective thermal quark mass of the order of gT. Hence, dileptons are generated by the annihilation of collective quark modes instead of bare quarks. In particular, the HTL quark dispersion contains a so-called plasmino branch, which exhibits a minimum at finite momentum. This nontrivial dispersion leads to sharp structures (van Hove singularities and energy gap) in the dilepton production rate[2] in contrast to the smooth Born rate. Second, the imaginary part of the HTL quark self-energy containing effective HTL N-point (propagators and quark-photon vertex) functions corresponds to processes involving the absorption or emission of thermal gluons.

In Fig. 1, the one-loop dilepton rate for zero momentum, containing such processes, is displayed as a function of the scaled invariant mass with the thermal quark mass and is also compared with the Born rate. In the left panel [Fig. 1(a)], the van Hove singularities due to the nontrivial dispersion of quarks in a medium are evident in pole-pole contributions, whereas the pole-cut and cut-cut contributions[3] are smooth, representing absorption and emission of gluons in the medium. The right panel [Fig. 1(b)] displays the total one-loop contribution for a set of values of g, where the energy gaps are smoothed by the pole-cut and cut-cut contributions. Also, the structures due to the van Hove singularities become also less prominent in the total contributions. The HTL rate, in particular, due to the cut contributions, is also singular at $M \to 0$ because the HTL quark-photon vertex is inversely proportional to photon energy.

However, these corrections are not sufficient, and two-loop diagrams within the HTL perturbation scheme contribute to the

[1]Note that for ultrasoft $M \sim g^2T$ and arbitrary momentum, the rate is nonperturbative and cannot be calculated even within the HTL improved perturbation theory. This observation holds in particular for real hard photons [27].

[2]For a discussion of van Hove singularities in the QGP, see Refs. [28–30] for $\vec{\mathbf{p}} = 0$ and Ref. [31] for $\vec{\mathbf{p}} \neq 0$.

[3]These are due to the spacelike ($k^2 > k_0^2$) part of the N-point HTL functions that acquire a cut contribution from below the light cone.

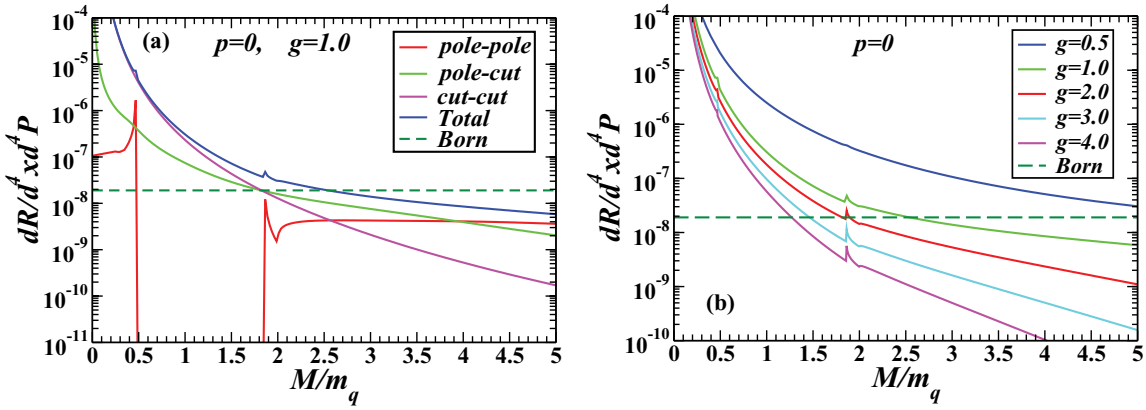

FIG. 1. (Color online) Left panel (a): One-loop dilepton rate for small invariant masses $M \sim gT$ at zero momentum and Born rate (dashed line) vs the scaled invariant photon mass M/m_q for $g = 1$. The van Hove peaks and energy gap are evident in the one-loop rate. Right panel (b): Total one-loop rate for various g values.

same order and are even larger than the one-loop results [16]. The total one- and two-loop rate at $\vec{\mathbf{p}} = 0$ and $M \ll T$ in the leading logarithm, that is, $\ln(1/g)$ approximation reads [16,32]

$$\frac{dR}{d^4x d^4P} = \frac{5\alpha^2}{9\pi^6}\frac{m_q^2}{M^2}\left[\frac{\pi^2 m_q^2}{4M^2}\ln\frac{T^2}{m_q^2} + \frac{3m_q^2}{M^2}\ln\frac{T^2}{m_g^2} + \frac{\pi^2}{4}\ln\left(\frac{MT}{M^2+m_q^2}\right) + 2\ln\left(\frac{MT}{M^2+m_g^2}\right)\right], \tag{5}$$

where the thermal gluon mass is given by $m_g^2 = 8m_q^2/3$ with $m_q = gT/\sqrt{6}$. Note that this expression is of the same order in g as the Born term for soft $M \sim gT$. Now, the Born term for $\vec{\mathbf{p}} = 0$ and $M \ll T$ is simply given by

$$\frac{dR}{d^4x d^4P} = \frac{5\alpha^2}{144\pi^4} = 1.90 \times 10^{-8}. \tag{6}$$

In Fig. 2, the Born rate and the complete two-loop rate for a set of values of g are compared. It is evident from Fig. 2 that

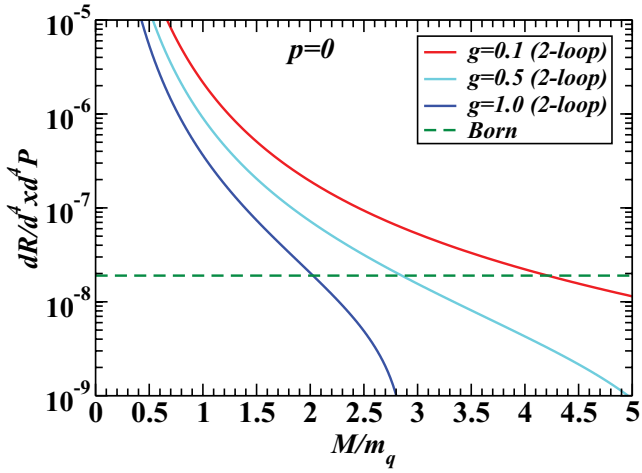

FIG. 2. (Color online) Complete two-loop dilepton rate for small invariant masses $M \sim gT$ at zero momentum and Born rate (dashed line) vs the scaled invariant photon mass M/m_q with the thermal quark mass m_q.

the two-loop rate dominates in the perturbative regime ($g \leqslant 1$) over the Born term for a low-mass domain, $M/m_q \leqslant 2$. However, the van Hove singularities contained in one loop do not appear, because they are washed out as a result of the leading logarithm approximation within the two-loop HTLpt.

2. Semihard rate ($M \sim T$ and $p \gg T$)

For M of the order of T and hard momenta ($p \gg T$), the α_s correction to the Born rate has been calculated [33] within the HTLpt method as

$$\frac{dR}{d^4x d^4P} = \frac{5\alpha^2\alpha_s}{27\pi^3}\frac{T^2}{M^2}e^{-E/T}\left(\ln\frac{T(m_q+k^*)}{m_q^2} + C\right), \tag{7}$$

where $k^* \approx |Em_q^2/M^2 - m_q^2/(4E)| < (E+p)/2$ and $C \approx -0.5$ depends weakly on M. In Ref. [34], it has been shown that further corrections to the rate (7) are necessary. However, numerical results showed only a slight modification.

Assuming typical values of the strong coupling constant and temperature, $T = 200$ MeV, these corrections dominate over the Born term for invariant masses below 300 MeV as shown in Fig. 3. Similar results have been obtained using bare quark propagators [35]. However, the calculation within naive perturbation theory [36] resulted in α_s corrections that are of similar size as the Born rate in the regime M and p of the order of T.

3. Hard rate ($M \gg T$)

For $M \gg T$, naive perturbation theory using bare propagators and vertices is sufficient. This is in contrast to the production of real photons, where one encounters an infrared singularity from bare quark propagator [37]. For finite M, however, this singularity cancels [38]. Bare two-loop calculations [36,38] showed that the α_s corrections are negligible in this regime. However, a recent calculation of the α_s corrections [39] for large invariant mass $M \gg T$ and small momenta $p \ll T$ yielded important corrections to the Born rate for invariant masses below $(2-3)T$. However, this work has also been criticized [40].

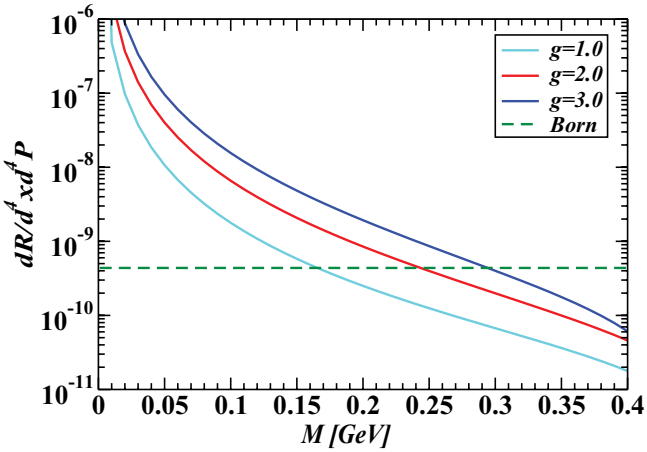

FIG. 3. (Color online) The α_s correction to the dilepton rate and Born rate (dashed line) vs the invariant photon mass M scaled with the thermal quark mass for $T = 200$ MeV and $E = 1$ GeV.

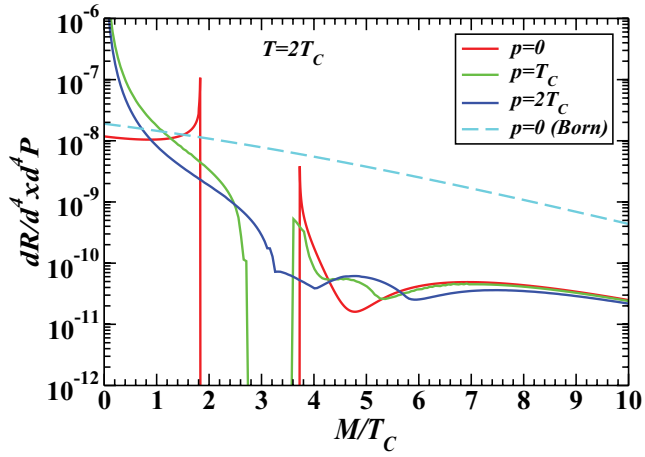

FIG. 4. (Color online) Van Hove singularities in the dilepton rate in the presence of gluon condensate as a function of invariant mass scaled with T_c for a set of momenta at $T = 2T_c$. The dashed curve is for the Born rate at zero momentum.

The main problem in applying the perturbative results discussed previously to realistic situations is the fact that g is not small; rather we have $g \sim 1.5$–2.5. Close to the critical temperature, T_c, even g could be as high as 6 [41]. Hence, the different momentum scales are not distinctly separated in the real sense and, even if one still believes in perturbative results (see Figs. 1, 2, and 3) at least qualitatively, it is not clear which of these rates applies to heavy-ion collisions. However, in all cases, there are substantial corrections to the Born rate. The perturbative rates within their uncertainties in various regime probably suggest that the Born rate may not be sufficient for describing the low-mass dilepton spectrum.

C. Nonperturbative rate

Considering the uncertainty of thermal perturbation theory for QCD, a nonperturbative approach to the dilepton rate would be desirable. In this subsection, we describe nonperturbative dilepton production rates in a deconfined phase in phenomenological models and in a first-principle calculation, viz., within the lattice gauge theory.

1. Rate using gluon condensate within the Green function

An important issue in understanding the phase structure of QCD is to understand the various condensates, which serve as order parameters of the broken symmetry phase. These condensates are nonperturbative in nature, and lattice provides a connection with bulk properties of QCD matter. However, the quark condensate has a rather small impact on the bulk properties (e.g., on the equation of state of QCD matter) compared to the gluon condensate [18]. The relation of the gluon condensate to the bulk properties such as equation of states, in principle, can be tested through hydrodynamic or transport properties sensitive to the equation of states, but this is a nontrivial task.

A semiempirical way to consider nonperturbative aspects (e.g., gluon condensate) has been suggested by combining lattice results with the Green function in momentum space [42,43]. In this approach, the effective N-point functions [42,43] have been constructed, which contain the gluon condensate in the deconfined phase, measured in lattice QCD [18]. The resulting quark dispersion relation with a mass $m_q \sim 1.15T_c$ [42] in the medium shows qualitatively the same behavior as the HTL dispersion, leading again to sharp structures (van Hove singularities, energy gap) in the dilepton production rates [44], indicating that this features are universal in relativistic plasmas independent of the approximation used [29]. In Fig. 4, the dilepton production rate using gluon condensate is displayed for various values of momentum at $T = 2T_c$ and also compared with the Born rate. At very low invariant mass ($M/T_c \leqslant 2$; for $T_c \sim 165$ MeV, $M \leqslant 330$ MeV) with realistic momentum, the dilepton rate with gluon condensate dominates over the Born rate. This rate will be important at very low invariant mass as it has nonperturbative input from lattice QCD that describes the bulk properties of the deconfined phase and is of course free from any uncertainty related to the strong coupling g associated with the perturbative rates discussed in Sec. II B.

However, we also note that the rate deviates from the Born rate at high M/T_c ($\geqslant 4$). The difference at high M/T_c has the origin in the asymptotic limit (large momentum k) of the quark dispersion relation with gluon condensates. In this limit, it is found that the normal quark mode behaves like $w_+ = k + c$, where c contains still the nonzero contribution from the condensates. The reason for this is the use of the momentum-independent condensate values. This fact has crept in the dilepton rate at high M/T_c. One way out could be to use an *ad hoc* separation scale ($M/T_c \sim 2$–3) up to which one may employ the nonperturbative quark dispersion associated with the gluon condensate and beyond which a free dispersion is adopted. Alternatively, one could use a momentum-dependent condensate, which is again beyond the scope of our calculation and has to be provided by the lattice analysis. To date we are not aware of such analysis. Nonetheless, we note that the nonperturbative contribution is important only at low invariant mass, as we see in Sec. III.

2. *Quark and ρ^0 meson interaction (ρ meson in QGP)*

We assume that ρ-meson-like states ($q\bar{q}$ correlator in the ρ-meson channel) can exist in a deconfined phase like QGP. Then there will also be a contribution from ρ-meson channel to the dilepton pairs (l^+l^-) in addition to the perturbative production. To consider such a channel phenomenologically, an interaction of ρ-q coupling is introduced through the Lagrangian [45]

$$\mathcal{L} = -\frac{1}{4}\rho^a_{\mu\nu}\rho^{\mu\nu}_a + \frac{1}{2}m_\rho^2\rho^a_\mu\rho^\mu_a + \bar{q}\left(i\gamma_\mu\partial^\mu - m_q + G_\rho\gamma^\mu\frac{\tau_a}{2}\rho^a_\mu\right)q, \tag{8}$$

where q is the quark field, m_q is the quark mass, a is the isospin or flavor index, and τ_a is the corresponding isospin matrix. The ρ-q coupling, G_ρ, can be obtained in the same spirit as the four-point interaction, $G_2(\bar{q}\gamma_\mu\tau_a q)^2$, in the Nambu-Jona-Lasinio (NJL) model. This suggests $G_\rho = \sqrt{8m_\rho^2 G_2} \sim 6$, by taking G_2 from the literature. The similar value for G_ρ can be obtained by simply assuming that the ρ meson couples in a universal way to nucleons, pions, and quarks [45].

Now, using the vector meson dominance (VMD) [25], the photon self-energy is related to the ρ^0 meson propagator, $D_{\mu\nu}(P)$, by

$$\mathrm{Im}\,\Pi^\mu_\mu(P) = \frac{e^2}{G_\rho^2}m_\rho^4\,\mathrm{Im}\,D^\mu_\mu(P). \tag{9}$$

Then the thermal dilepton production rate from the ρ meson can be written as

$$\frac{dR}{d^4x\,d^4P} = -\frac{1}{3\pi^3}\frac{\alpha^2}{G_\rho^2}\frac{m_\rho^4}{M^2}\frac{1}{e^{E_P/T}-1}\left(\mathcal{A}_\rho^L + 2\mathcal{A}_\rho^T\right), \tag{10}$$

and the spectral functions for the ρ meson can be obtained from the self-energy of the ρ meson as

$$\mathcal{A}_\rho^L(P) = \frac{\mathrm{Im}\,\mathcal{F}}{\left(M^2 - m_\rho^2 - \mathrm{Re}\,\mathcal{F}\right)^2 + (\mathrm{Im}\,\mathcal{F})^2}, \tag{11}$$

$$\mathcal{A}_\rho^T(P) = \frac{\mathrm{Im}\,\mathcal{G}}{\left(M^2 - m_\rho^2 - \mathrm{Re}\,\mathcal{G}\right)^2 + (\mathrm{Im}\,\mathcal{G})^2}, \tag{12}$$

where $\mathcal{F} = -\frac{P^2}{p^2}\Pi^{00}(P)$ and $\mathcal{G} = \Pi_T(P)$ with L and T standing for longitudinal and transverse modes, respectively.

Going beyond the HTL approximation, the integral expression for the matter part of the one-loop photon self-energy for asymmetric charges in the deconfined phase (viz., with nonzero chemical potential, μ, which would be appropriate for FAIR energies [22]) can be obtained easily by extending the results of Ref. [45] to finite μ as

$$\begin{aligned}
\mathrm{Re}\,\mathcal{F} &= \frac{3G^2}{4\pi^2}\frac{M^2}{p^2}\int_0^\infty dk\,k\,[n(\omega_k-\mu)+n(\omega_k+\mu)]\left(-2\frac{k}{\omega_k} + \frac{M^2+4\omega_k^2}{4p\omega_k}\ln|a| + \frac{p_0}{p}\ln|b|\right),\\
\mathrm{Im}\,\mathcal{F} &= \frac{3G^2}{4\pi}\frac{M^2}{p^3}\int_{k_-}^{k_+} dk\,k\,[n(\omega_k-\mu)+n(\omega_k+\mu)]\left(p_0 - \omega_k - \frac{M^2}{4\omega_k}\right),\\
\mathrm{Re}\,\mathcal{G} &= \frac{3G^2}{4\pi^2}\int_0^\infty dk\,\frac{k^2}{\omega_k}\,[n(\omega_k-\mu)+n(\omega_k+\mu)]\left(-\left[\frac{\omega_k^2M^2}{2p^3k} + \frac{M^2}{4pk} + \frac{M^4}{8p^3k} + \frac{m_q^2}{2pk}\right]\ln|a| - \frac{p_0M^2\omega_k}{2p^3k}\ln|b| + \frac{M^2}{p^2} + 2\right),\\
\mathrm{Im}\,\mathcal{G} &= \frac{3G^2}{8\pi p}\int_{k_-}^{k_+} dk\,k\;\;[n(\omega_k-\mu)+n(\omega_k+\mu)]\left(-\omega_k + \frac{m_q^2}{\omega_k} + \frac{p_0^2}{p^2}\omega_k + \frac{M^2}{2\omega_k} + \frac{M^4}{4\omega_k p^2} - \frac{p_0M^2}{p^2}\right),
\end{aligned} \tag{13}$$

along with

$$a = \frac{(M^2+2pk)^2 - 4p_0^2\omega_k^2}{(M^2-2pk)^2 - 4p_0^2\omega_k^2}, \quad b = \frac{M^4 - 4(pk+p_0\omega_k)^2}{M^4 - 4(pk-p_0\omega_k)^2},$$

$$k_- = \frac{1}{2}\left|p_0\sqrt{1-\frac{4m_q^2}{M^2}} - p\right|, k_+ = \frac{1}{2}\left(p_0\sqrt{1-\frac{4m_q^2}{M^2}} + p\right),$$

where $\omega_k = \sqrt{k^2+m_q^2}$.

In Fig. 5, the ρ-meson spectral function related to the imaginary part of the ρ-meson propagator (left panel) in (9) and the dilepton rate (right panel) are displayed for various temperatures with $\mu = 0$ and $p = 200$ MeV. As the temperature increases, the peak in the imaginary part of the ρ-meson propagator D becomes broader and is also reflected in the dilepton rate. In the low-mass region ($\leqslant$1 GeV), the rate is comparable with the Born rate.

In Fig. 6, the ρ-meson spectral function (left panel) and the dilepton rate (right panel) are displayed for various μ at $T = 160$ MeV and $p = 200$ MeV, which could be appropriate in the perspective of FAIR energies. The effect of broadening of the ρ meson is far less pronounced with increasing μ than increasing T, indicating that the ρ meson is not completely melted in the case of a system with finite baryon density such as expected at FAIR energies even above the phase transition. However, dilepton rates from the ρ meson as shown in Figs. 5 and 6 are comparable with the Born rate in QGP in the low-mass region ($M \leqslant 1$ GeV) and may be an indication for chiral restoration [10,11,45]. In addition, this rate would be important for invariant masses below 1 GeV.

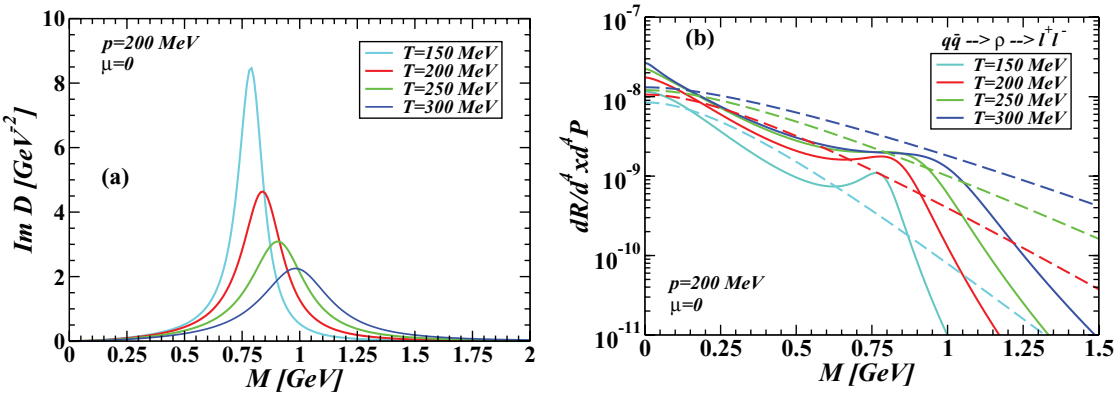

FIG. 5. (Color online) Left panel (a): Imaginary part of ρ-meson propagator (spectral function) as a function of the invariant mass M for a set of values T. Right panel (b): The dilepton rate from the ρ meson in a QGP as a function of M. The dashed lines are the corresponding Born rates. We have used $G_\rho = 6$.

We also note that if one includes higher mass vector mesons such as ϕ meson within VMD, then there will be a peak corresponding to an invariant mass of the order of ϕ-meson mass, but in the low-mass region ($M \leqslant 1$ GeV) there should be a very little change (less than 5%) in the dilepton rate. Because we are interested in the low-mass region, we have not discussed the ϕ meson here.

3. Rate from lattice gauge theory

The thermal dilepton rate describing the production of lepton pairs with energy ω and momentum $\vec{\mathbf{p}}$ is related to the Euclidian correlation function [30] of the vector current, $J_V^\mu = \bar{\psi}(\tau, \vec{\mathbf{x}})\gamma^\mu \psi(\tau, \vec{\mathbf{x}})$, which can be calculated numerically in the framework of lattice gauge theory. The thermal two-point vector correlation function in coordinate space, $\mathcal{G}_V(\tau, \vec{\mathbf{x}})$, is defined as

$$\mathcal{G}_V(\tau, \vec{\mathbf{x}}) = \langle J_V(\tau, \vec{\mathbf{x}}) J_V^\dagger(\tau, \vec{\mathbf{x}}) \rangle = T \sum_{n=-\infty}^{\infty} \int \frac{d^3p}{(2\pi)^3} e^{-i(w_n\tau - \vec{\mathbf{p}}\cdot\vec{\mathbf{x}})} \chi_V(w_n, \vec{\mathbf{p}}), \quad (14)$$

where the Euclidian time τ is restricted to the interval $[0, \beta = 1/T]$, and the Fourier transformed correlation function χ_V is given at the discrete Matsubara modes, $w_n = 2\pi nT$. The imaginary part of the momentum space correlator gives the spectral function $\sigma_V(\omega, \vec{\mathbf{p}})$, as

$$\chi_V(w_n, \vec{\mathbf{p}}) = -\int_{-\infty}^{\infty} \frac{\sigma_V(\omega, \vec{\mathbf{p}})}{i w_n - \omega + i\epsilon} \Rightarrow \sigma_V(\omega, \vec{\mathbf{p}}) = \frac{1}{\pi} \text{Im}\, \chi_V(\omega, \vec{\mathbf{p}}). \quad (15)$$

Using Eqs. (14) and (15), we can obtain the spectral representation of the thermal correlation functions at fixed momentum in coordinate space as

$$\mathcal{G}(\tau, \vec{\mathbf{p}}) = \int_0^\infty d\omega\, \sigma_V(\omega, \vec{\mathbf{p}}) \frac{\cosh[\omega(\tau - \beta/2)]}{\sinh[\omega\beta/2]}. \quad (16)$$

The vector spectral function, σ_V, is related to the differential dilepton production rate [30][4] as

$$\sigma_V(\omega, \vec{\mathbf{p}}) = \frac{18\pi^2 N_c}{5\alpha^2} \omega^2 \, (e^{\omega/T} - 1) \frac{dR}{d^4x d^4P}, \quad (17)$$

where N_c is the number of color degrees of freedom.

[4] A factor of 2 differs from that of Ref. [17]

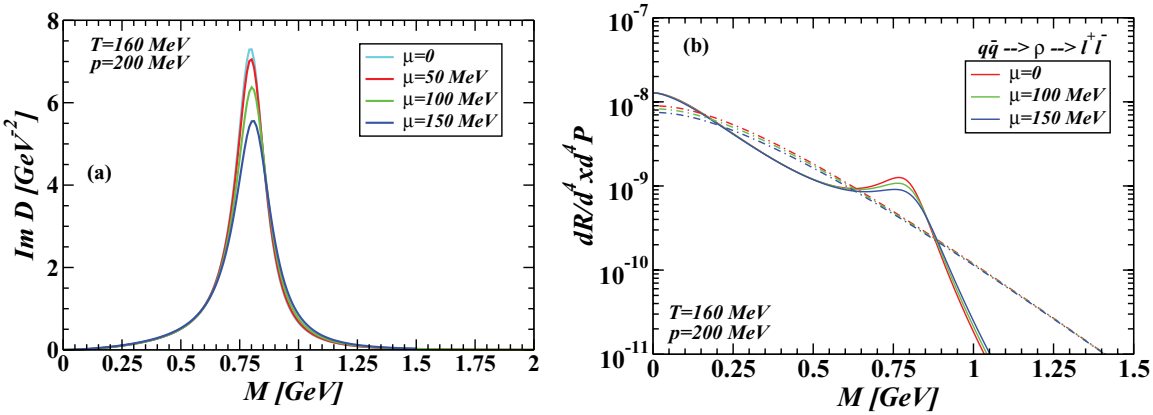

FIG. 6. (Color online) Same as Fig. 5 but for different μ at a given T.

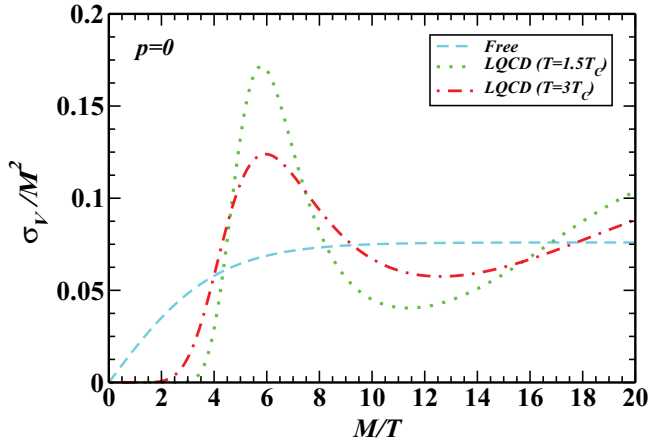

FIG. 7. (Color online) Zero-momentum ($\vec{\mathbf{p}} = 0$) vector spectral function, reconstructed from the correlation function [17] within lattice gauge theory in quenched QCD using MEM, scaled with M^2 as a function of M/T compared with that of the free one above the deconfinement temperature T_c.

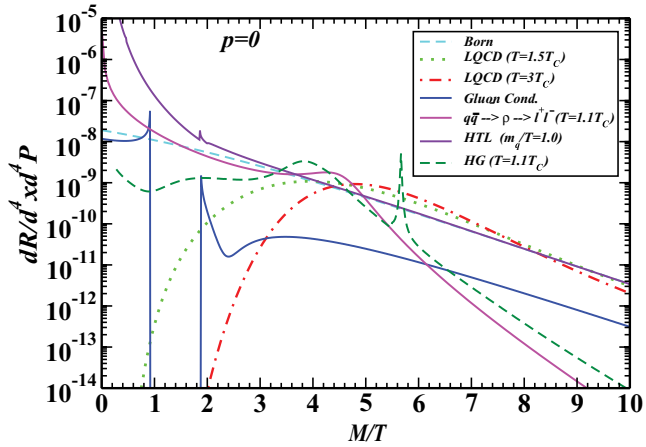

FIG. 8. (Color online) Comparison of various dilepton rates in a QGP and in HG as a function of M/T for momentum $\vec{\mathbf{p}} = 0$. The critical temperature is 165 MeV [20], and the value of G_ρ is chosen as 6. The in-medium HG rate is from the recent calculations of Ref. [48].

A finite-temperature lattice gauge theory calculation is performed on lattices with finite temporal extent N_τ, which provides information on the temporal correlation function, $\mathcal{G}(\tau, \vec{\mathbf{p}})$, only for a discrete and finite set of Euclidian times $\tau = k/(N_\tau T)$, $k = 1, \ldots, N_\tau$. The correlation function, $\mathcal{G}(\tau, \vec{\mathbf{p}})$, has been computed [17] within the quenched approximation of QCD using nonperturbative improved clover fermions [46] through a probabilistic application based on the maximum entropy method (MEM) [47] for temporal extent $N_\tau = 16$ and spatial extent $N_\sigma = 64$. Then by inverting the integral in Eq. (16), the spectral function is reconstructed [17] in lattice QCD. In Fig. 7, such a reconstructed spectral function scaled with M^2 (equivalently ω^2 for $\vec{\mathbf{p}} = 0$) is displayed as a function of M/T. The vector spectral functions above the deconfinement temperature (viz., $T = 1.5T_c$ and $3T_c$) show an oscillatory behavior compared to the free one. The spectral functions are also found to be vanishingly small for $M/T \leqslant 4$ because of the sharp cutoff used in the reconstruction.

A direct calculation of the differential dilepton rate using Eq. (17) above the deconfined temperature (T_c) at $\vec{\mathbf{p}} = 0$ was first time done in Ref. [17] within the lattice gauge theory in quenched QCD using the MEM. In Fig. 8, the lattice dilepton rates at $\vec{\mathbf{p}} = 0$ for two temperatures ($T = 1.5T_c$ and $3T_c$) are displayed as a function of the scaled invariant mass with temperature and $M/T = \omega/T$, the energy of the dileptons. We have also compared the perturbative, nonperturbative, and in-medium hadron rates within the same normalization as shown in the plot. We note that the rate with gluon condensate perfectly scales with the temperature, whereas that of HTL depends on the choice of the effective coupling, $m_q/T \sim g/\sqrt{6}$. The lattice results are comparable within a factor of 2 with the Born rate as well as that of HTLpt at high invariant mass $M/T \geqslant 4$. The absence of peak structures around the ρ mass and also at higher M in the lattice dilepton rate probably constrain the broad resonance structures in the dilepton rates. However, for invariant mass below $M/T \leqslant 4$, the lattice dilepton rate falls off very fast. This is because the sharp cutoff is used to reconstruct the spectral function from the correlation function and the finite volume restriction in the lattice analysis. The lattice analysis is also based on rather small statistics. These lattice artifacts are related to the smaller invariant masses, which in turn indicate that it is not yet very clear whether there will be any low-mass thermal dileptons from the deconfined phase within the lattice gauge theory calculation. Future analysis could improve the situation in this low-mass regime. One cannot rule out [17] the existence of van Hove singularities and energy gap, which are general features of massless fermions in a relativistic plasma [29], in the low-mass dileptons. This calls for further investigation on the lattice gauge theory side by improving and refining the lattice ingredients and constraints.

On the other hand, in HTLpt, apart from the uncertainty in the choice of g, the low-mass ($M \to 0$, vanishing photon energy) one-loop dilepton rate obtained from vector meson spectral function analysis [30] diverges because the quark-photon vertex is inversely proportional to the photon energy. This also requires further improvement of the HTLpt. However, we assume that the perturbative rate could also be reliable for $M \geqslant 200$ MeV with $T \geqslant 200$ MeV and g of the order of 2. The other two phenomenological models, viz., gluon condensate measured in lattice [18] and ρ-q interaction in the deconfined phase, as discussed respectively in Secs. II C 1 and II C 2, for nonperturbative dilepton production at low-mass regime are at least cleaner than the perturbative rates, which depend weakly on the choice of the strong coupling constant. The rate with gluon condensate is free from strong coupling, whereas that from ρ-q interaction does not depend strongly on the choice of the coupling (see Fig. 9). In addition to the perturbative rate, these two together could also provide a realistic part of the dilepton rate at low-mass regime ($\leqslant 1$ GeV) from the deconfined phase, as also can be seen in the next section. As a comparison, we have also shown the recent rate from in-medium hadrons of Ref. [48], where the analytic

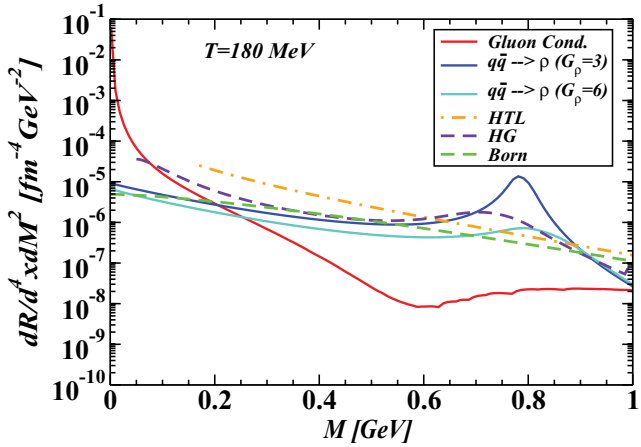

FIG. 9. (Color online) Momentum integrated dilepton rate as a function of the invariant mass M. We have used $T_c = 165$ MeV for the nonperturbative rate with gluon condensate. The in-medium hadronic rate (HG) is from Ref. [48].

structure of the ρ-meson propagator has been used because of its interaction with thermal mesons.

III. MOMENTUM INTEGRATED RATE

The momentum integrated dilepton rate can be obtained as

$$\frac{dR}{d^4x dM^2} = \int \frac{d^3p}{2p_0} \frac{dR}{d^4x d^4P}. \tag{18}$$

In Fig. 9, dilepton rates from QGP and in-medium hadrons are displayed as a function of invariant mass. As can be seen, the nonperturbative contribution using gluon condensate dominates over the Born rate as well as the perturbative rate below $M \leqslant 200$ MeV. The nonperturbative rate is indeed important with input from the first principle calculations [18] that describe the bulk properties of the deconfined phase. More important, this domain is also beyond reach of any reliable perturbative calculations in a true sense. The rate from the ρ-q interaction is almost of the same order as that of the Born rate as well as the in-medium hadrons for $M \leqslant 600$ MeV, whereas it is higher than the perturbative one in the domain $600 \leqslant M$ (MeV) $\leqslant 800$ due to the broadening of the ρ peak in the medium. We also note that this rate has a weak dependence on the realistic range of values of the ρ-q coupling (2–6). In addition, the higher order perturbative rate from HTL, as discussed previously, becomes reliable for $M \geqslant 200$ MeV and also becomes of the order of Born rate for $M \geqslant 500$ MeV. We also note that the momentum integrated HTL rate used here has been obtained recently by Rapp *et al.* [11] through a parametrization of the prefactor of the zero-momentum one-loop HTL rate [28] with a temperature-dependent g, which is claimed [49] to reproduce the Born rate in Eq. (2) within the appropriate limit. Now, for comparison, we have also shown the recent rate from the in-medium hadrons of Ref. [48]. It is clear that for low invariant mass ($\leqslant$1 GeV) only the Born rate from the QGP is unrealistic as well as insufficient for describing the dilepton rate. Instead, we suggest that the nonperturbative rate with gluon condensate should be important for $M \leqslant 200$ MeV, whereas the rates from the ρ-q interaction and HTLpt are important for $M \geqslant 200$ MeV. Next, we discuss some aspects of the quark-hadron duality hypothesis [23].

IV. THOUGHTS ON THE QUARK-HADRON DUALITY HYPOTHESIS

It is advocated [10,23] that because of the potential broadening of the ρ-meson resonance suffering in a dense hadronic environment, the overall (momentum integrated) dilepton rate out of the hadronic gas becomes equivalent to that from the deconfined phase as

$$\frac{dR_H}{d^4x dM^2} \approx \frac{dR_Q}{d^4x dM^2}, \tag{19}$$

which entails a reminiscence to a simple perturbative $q\bar{q}$ annihilation in the vicinity of the expected QGP phase transition. This hypothesis of extended quark-hadron duality for the thermal source of low-mass dileptons has been claimed as an indication for chiral symmetry restoration [10,11,23] in the deconfined phase. However, we note that in this hypothesis the volumes of QGP and hadronic gas was assumed to be the same in a given instant of time and therefore the dileptons shine equally bright from both phases at a given instant of time per unit volume. This aspect of quark-hadron duality should be carefully re-addressed on its general validity, as the suggestive conclusion is indeed far reaching. A more realistic way to look into it is envisaged here.

The momentum integrated rate in Eq. (18) should be gauged to the adequate degrees of freedom in a particular phase. A certain measure is given by the corresponding entropy density. Hence, we suggest that for duality to hold one approximately should have

$$\frac{1}{s_H}\frac{dR_H}{d^4x dM^2} \approx \frac{1}{s_Q}\frac{dR_Q}{d^4x dM^2}, \tag{20}$$

where s_i $(i = H, Q)$ is the entropy density of the respective phase. For an isoentropic crossing over the phase transition, one has $s_H dV_H \approx s_Q dV_Q$. Hence, if one takes into account the respective volume of both phases at a given instant of time, then instead of Eq. (19) one should ask for

$$dV_H \frac{dR_H}{d^4x dM^2} \approx dV_Q \frac{dR_H}{d^4x dM^2}, \tag{21}$$

where dV_i $(i = Q,\ H)$ is the volume of the respective phase. Now, at a given instant of time this can lead to

$$\frac{dR_H}{dt dM} \approx \frac{dR_Q}{dt dM}, \tag{22}$$

where $dR_i/dt dM$ is the total yield per time from total phase i in the system at any instant of time. Therefore, Eq. (22) means that the fireball emits the same number of dileptons per unit time if described either by a hadronic or by a deconfined partonic description. This could likely be a more realistic way to look into the quark-hadron duality. Now, even if the momentum integrated rates in Eq. (18) from both phases are

same in some kinematic domain (e.g., see Fig. 9), this may not necessarily imply a quark-hadron duality as given by (22) because the hadronic volume is expected to be larger than that of QGP by at least a factor of 4 to 5. Furthermore, we note that the quark-hadron duality should also be true for any momentum at a given instant of time.

V. CONCLUSION

We have discussed the low-mass dilepton production rate from the deconfined phase within various models, viz., perturbative and nonperturbative, and compared it with that of first-principle calculations based on lattice gauge theory and in-medium hadrons. We also have discussed in detail the limitations and uncertainties of all those models at various domains of the invariant mass. It turns out that at very low invariant mass ($\leqslant$200 MeV) the nonperturbative rate using gluon condensate measured in lattice becomes important as this domain is beyond reach of any reliable perturbative calculations. The other nonperturbative contribution from ρ-q interaction also becomes important below 1 GeV as it is almost of same order as those of the Born and in-medium hadrons. We also note that these two rates are at least cleaner than the perturbative rates, in the sense that the gluon condensate rate has nonperturbative input from lattice equation of states and is thus free from any coupling uncertainties, whereas the ρ-q interaction rate does not depend strongly on the choice of its coupling. We also discussed the ρ-q interaction in the perspective from the FAIR scenario.

On the other hand, the perturbative contribution, within its various uncertainties, becomes steady and reliable beyond $M > 200$ MeV and also becomes comparable with the Born rate and the lattice gauge theory rate for $M \geqslant 500$ MeV. The lattice gauge theory rate also constrains the broad resonance structure at large invariant mass. More specifically, the rate with gluon condensate is important for $M \leqslant 200$ MeV, whereas those from the ρ-q interaction and HTLpt would be important for $M \geqslant 200$ MeV for the deconfined phase in heavy-ion collisions. Instead of considering only the Born rate, the various nonperturbative and perturbative rates from appropriate domains of the invariant mass below 1 GeV would comprise a more realistic rate for low-mass dileptons from the deconfined phase created in heavy-ion collisions. We hope that more elaborate lattice gauge theory studies on dileptons above the deconfined temperature can provide more insight than the present lattice gauge theory calculations on the low-mass region, which could then verify the various model calculations on low-mass dileptons above the deconfined temperatures. Finally, we also have discussed a realistic way to look into the quark-hadron duality hypothesis.

ACKNOWLEDGMENTS

The authors are thankful to S. Sarkar for providing the result of their calculations for in-medium hadron gas rate and P. Petreczky for supplying the lattice data. M.G.M. acknowledges various useful discussions and communications with H. van Hees. This work was partly supported by the Helmholtz International Centre for FAIR within the framework of the LOEWE (Landes-Offensive zur Entwicklung Wissenschaftlich-ökonomischer Exzellenz) program launched by the state of Hesse, Germany.

[1] U. Heinz and M. Jacob, arXiv:nucl-th/0002042.
[2] I. Arsene *et al.* (BRAHMS Collaboration), Nucl. Phys. A **757**, 1 (2005); K. Adcox *et al.* (PHENIX Collaboration), *ibid.* **757**, 184 (2005); B. B. Back *et al.* (PHOBOS Collaboration), *ibid.* **757**, 28 (2005); J. Adams *et al.* (STAR Collaboration), *ibid.* **757**, 102 (2005).
[3] A. Adare *et al.* (PHENIX Collaboration), Phys. Rev. C **81**, 034911 (2010).
[4] S. S. Adler *et al.* (PHENIX Collaboration), Phys. Rev. Lett. **98**, 012002 (2007).
[5] A. Adare *et al.* (PHENIX Collaboration), Phys. Rev. Lett. **98**, 162301 (2007).
[6] K. Adcox *et al.* (PHENIX Collaboration), Phys. Rev. Lett. **88**, 022301 (2002); C. Adler *et al.* (STAR Collaboration), *ibid.* **89**, 092302 (2002).
[7] S. S. Adler *et al.* (PHENIX Collaboration), Phys. Rev. Lett. **91**, 172301 (2003); T. Chujo (PHENIX Collaboration), Nucl. Phys. A **715**, 151c (2003).
[8] L. D. McLerran and T. Toimela, Phys. Rev. D **31**, 545 (1985).
[9] G. Agakichiev *et al.* (CERES Collaboration), Phys. Rev. Lett. **75**, 1272 (1995); Phys. Lett. B **422**, 405 (1998); N. Masera (HELIOS-3 Collaboration), Nucl. Phys. A **590**, 93c (1995); A. Drees (CERES Collaboration), Nucl. Phys. B **630**, 449c (1998).
[10] R. Rapp and J. Wambach, Adv. Nucl. Phys. **25**, 1 (2000).
[11] R. Rapp, J. Wambach, and H. van Hees, arXiv:0901.3289.
[12] W. Cassing and E. L. Bratkovskaya, Phys. Rep. **308**, 65 (1999).
[13] G. E. Brown and M. Rho, Phys. Rev. Lett. **66**, 2720 (1991); B. Friman and H. J. Priner, Nucl. Phys. A **617**, 496 (1997); R. Rapp, G. Chanfray, and J. Wambach, *ibid.* **617**, 472 (1997); G. Chanfray, R. Rapp, and J. Wambach, Phys. Rev. Lett. **76**, 368 (1996); C. Gale and P. Lichard, Phys. Rev. D **49**, 3338 (1994); R. Rapp and C. Gale, Phys. Rev. C **60**, 024903 (1999); F. Klingl, N. Kaiser, and W. Wiese, Nucl. Phys. A **624**, 527 (1997); W. Peters, M. Post, H. Lenske, S. Leupold, and U. Mosel, *ibid.* **632**, 109 (1998); W. Cassing, E. L. Bratkovskaya, R. Rapp, and J. Wambach, Phys. Rev. C **57**, 916 (1998); M. Post, S. Leupold, and U. Mosel, Nucl. Phys. A **689**, 753 (2001); V. Koch, M. Bleicher, A. K. Dutt-Mazumder, C. Gale, and C. M. Ko, in *Hirschegg 2000: Hadrons in Dense Matter*, p. 136; D. K. Srivastava, B. Sinha, and C. Gale, Phys. Rev. C **53**, R567 (1996); D. Pal, K. Haglin, and D. K. Srivastava, *ibid.* **54**, 1366 (1996); D. K. Srivastava, B. Sinha, D. Pal, C. Gale, and K. Haglin, Nucl. Phys. A **610**, 350c (1996); D. Pal and M. G. Mustafa, Phys. Rev. C **60**, 034905 (1999); D. K. Srivastava, M. G. Mustafa, and B. Müller, *ibid.* **56**, 1064 (1997); J. Alam, S. Sarkar, P. Roy, T. Hatsuda, and B. Sinha, Ann. Phys.

286, 159 (2001); J. Alam, P. Roy, S. Sarkar, and B. Sinha, Phys. Rev. C **67**, 054901 (2003).
[14] K. Dusling and I. Zahed, Nucl. Phys. A **825**, 212 (2009).
[15] E. L. Bratkovskaya, W. Cassing, and O. Linnyk, Phys. Lett. B **670**, 428 (2009).
[16] P. Aurenche, F. Gelis, H. Zaraket, and R. Kobes, Phys. Rev. D **58**, 085003 (1998).
[17] F. Karsch, E. Laermann, P. Petreczky, S. Stickan, and I. Wetzorke, Phys. Lett. B **530**, 147 (2002).
[18] G. Boyd *et al.*, Nucl. Phys. B **469**, 419 (1996).
[19] C. R. Allton, S. Ejiri, S. J. Hands, C. Kaczmarek, F. Karsch, E. Laermann, and C. Schmidt, Phys. Rev. D **68**, 014507 (2003); C. R. Allton, M. Doring, S. Ejiri, S. J. Hands, C. Kaczmarek, F. Karsch, E. Laermann, and K. Redlich, *ibid.* **71**, 054508 (2005); A. Bazavov *et al.*, *ibid.* **80**, 014504 (2009); C. Bernard *et al.* (MILC Collaboration), *ibid.* **71**, 034504 (2005).
[20] P. Petreczky, Nucl. Phys. A **830**, 11c (2009); Mod. Phys. Lett. A **25**, 3081 (2010).
[21] M. H. Thoma, J. Phys. G **31**, L7 (2005).
[22] [http://www.gsi.de/forschung/fair_experiments/CBM/index_e.html].
[23] R. Rapp and J. Wambach, Eur. Phys. J. A **6**, 415 (1999).
[24] J. Cleymans, J. Fingberg, and K. Redlich, Phys. Rev. D **35**, 2153 (1987).
[25] C. Gale and J. Kapusta, Nucl. Phys. B **357**, 65 (1991).
[26] E. Braaten and R. D. Pisarski, Nucl. Phys. B **337**, 569 (1990); Phys. Rev. Lett. **64**, 1338 (1990).
[27] P. Aurenche, F. Gelis, and H. Zaraket, Phys. Rev. D **61**, 116001 (2000).
[28] E. Braaten, R. D. Pisarski, and T. C. Yuan, Phys. Rev. Lett. **64**, 2242 (1990).
[29] M. H. Thoma, Nucl. Phys. B, Proc. Suppl. **92**, 162 (2001); M. G. Mustafa and M. H. Thoma, Pramana **60**, 711 (2003); A. Peshier and M. H. Thoma, Phys. Rev. Lett. **84**, 841 (2000).
[30] F. Karsch, M. G. Mustafa, and M. H. Thoma, Phys. Lett. B **497**, 249 (2001).
[31] S. M. H. Wong, Z. Phys. C **53**, 465 (1992).
[32] P. Aurenche, F. Gelis, H. Zaraket, and R. Kobes, Phys. Rev. D **60**, 076002 (1999).
[33] M. H. Thoma and C. T. Traxler, Phys. Rev. D **56**, 198 (1997).
[34] M. E. Carrington, A. Gynther, and P. Aurenche, Phys. Rev. D **77**, 045035 (2008); P. Aurenche, F. Gelis, G. D. Moore, and H. Zaraket, J. High Energy Phys. 12 (2002) 006; 07 (2002) 063.
[35] T. Altherr and P. V. Ruuskanen, Nucl. Phys. B **380**, 377 (1992).
[36] J. Cleymans, I. Dadic, and J. Joubert, Phys. Rev. D **49**, 230 (1994); J. Cleymans and I. Dadic, *ibid.* **47**, 160 (1993).
[37] J. Kapusta, P. Lichard, and D. Seibert, Phys. Rev. D **44**, 2774 (1991); R. Baier, H. Nakkagawa, A. Niegawa, and K. Redlich, Z. Phys. C **53**, 433 (1992).
[38] T. Altherr and P. Aurench, Z. Phys. C **45**, 99 (1989).
[39] J. I. Kapusta and S. M. H. Wong, Phys. Rev. C **62**, 027901 (2000).
[40] P. Aurenche *et al.*, Phys. Rev. D **65**, 038501 (2002).
[41] A. Peshier, B. Kämpfer, O. P. Pavlenko, and G. Soff, Phys. Lett. B **337**, 235 (1994); Phys. Rev. D **54**, 2399 (1996); U. Heinz and P. Levai, Phys. Rev. C **57**, 1879 (1998).
[42] A. Schäfer and M. H. Thoma, Phys. Lett. B **451**, 195 (1999).
[43] M. G. Mustafa, A. Schäfer, and M. H. Thoma, Phys. Lett. B **472**, 402 (2000).
[44] M. G. Mustafa, A. Schäfer, and M. H. Thoma, Phys. Rev. C **61**, 024902 (1999); Nucl. Phys. A **661**, 653 (1999).
[45] M. H. Thoma, S. Leupold, and U. Mosel, Eur. Phys. J. A **7**, 219 (2000).
[46] B. Sheikholeslami and R. Wohlert, Nucl. Phys. B **259**, 572 (1985); M. Lüster *et al.*, *ibid.* **491**, 344 (1997).
[47] Y. Nakahara, M. Asakawa, and T. Hatsuda, Phys. Rev. D **60**, 091503 (1999); M. Asakawa, T. Hatsuda, and Y. Nakahara, Prog. Part. Nucl. Phys. **46**, 459 (2001); I. Wetzorke and F. Karsch, in *Proceedings of the International Workshop on Strong and Electroweak Matter*, edited by C. P. Korthals-Altes (World Scientific, Singapore, 2001), p. 193.
[48] S. Ghosh, S. Sarkar, and J. Alam, arXiv:1009.1260.
[49] H. van Hees (private communication).